Published in final edited form as:
ACS Chem Biol. 2010 April 16; 5(4): 359–364. doi:10.1021/cb100003r.

A semisynthesis platform for investigating structure-function relationships in the N-terminal domain of the anthrax lethal factor

Brad L. Pentelute[†], **Adam P. Barker**[†], **Blythe E. Janowiak**[†], **Stephen B. H. Kent**[‡], and **R. John Collier**[†,*]

[†]Department of Microbiology and Molecular Genetics, Harvard Medical School, Boston, Massachusetts 02115

[‡]Department of Chemistry, University of Chicago, Chicago, IL 60637

Abstract

Many bacterial toxins act by covalently altering molecular targets within the cytosol of mammalian cells and therefore must transport their catalytic moieties across a membrane. The Protective-Antigen (PA) moiety of anthrax toxin forms multimeric pores that transport the two enzymatic moieties, the Lethal Factor (LF) and the Edema Factor, across the endosomal membrane to the cytosol. The homologous PA-binding domains of these enzymes contain N-terminal segments of highly charged amino acids that are believed to enter the pore and initiate N- to C-terminal translocation. Here we describe a semisynthesis platform that allows chemical control of this segment in LF_N, the PA-binding domain of LF. Semisynthetic LF_N was prepared in milligram quantities by native chemical ligation of synthetic LF_N^{14-28} αthioester with recombinant N29C-LF_N^{29-263} and compared with two variants containing alterations in residues 14-28 of the N-terminal region. The properties of the variants in blocking ion conductance through the PA pore and translocating across planar phospholipid bilayers in response to a pH gradient were consistent with current concepts of the mechanism of polypeptide translocation through the pore. The semisynthesis platform thus makes new analytical approaches available to investigate the interaction of the pore with its substrates.

Anthrax lethal toxin is comprised of a receptor-binding, pore-forming moiety, termed Protective Antigen (PA; 83 kDa), and an enzymatic moiety, termed the Lethal Factor (LF; 90 kDa), which acts within the cytosol of mammalian cells (1). PA binds receptors ANTXR1 (2) or ANTXR2 (3) on host cells and is cleaved by a furin-family protease into two fragments, PA_{20} and PA_{63} (4,5). PA_{63} self-assembles into a ring-shaped heptamer (6) or octamer (7) to form a receptor-bound prepore. The heptamer binds up to three molecules of LF, and the octamer up to four, forming a series of complexes that are then endocytosed (8). Acidification within the endosome triggers conversion of the PA prepore to a membrane-spanning, ion-conductive pore (1), which transports bound LF from the endosome to the cytosol (9). A similar series of events leads to the entry of the Edema Factor, the enzymatic moiety of anthrax edema toxin.

For both lethal toxin and edema toxin, the N-terminal domain of the enzymatic moiety interacts with the pore and initiates translocation of the protein (Figure 1) (10). LF_N^{1-263}, the N-terminal domain of LF, has nanomolar binding affinity for the pore, and this domain

*Corresponding author, jcollier@hms.harvard.edu.

alone has proven to be a useful reagent to probe translocation (10). LF_N^{1-263} is a cysteine-free, globular, largely alpha-helical domain with an unstructured N-terminal segment (residues 1-30) carrying a high density of charged residues. Deleting the N-terminal 13 residues had little effect on translocation of the protein across the membrane, but deleting the first 27 residues hindered both its translocation and its ability to block ion conductance through the PA_{63} pore (10). These functions were in part restored by attaching a polycationic tract of amino acids to the N-terminus of truncated analogues of LF_N, implying that positive charge plays an important role in the interaction of the unstructured region of the native protein with the pore (10). However, much remains to be learned about the mechanism by which the unstructured N-terminal region of LF initiates translocation.

Protein semisynthesis is a versatile way to probe the structure and function of proteins (11). A semisynthesis involves establishing chemical control over a region within the protein while obtaining the remainder from natural or recombinant sources. With semisynthetic access, the protein can be modified in ways that are difficult or impossible by recombinant DNA methods; for instance, nonnatural amino acids can be incorporated or modifications to the backbone made.

A robust and reliable method for the chemical synthesis of proteins entails the use of native chemical ligation–a chemoselective reaction between a peptide-thioester and a Cys-peptide (12). In this paper, we have used native chemical ligation to prepare analogues of LF_N^{14-263} (Figure 2) according to a protocol that allowed chemical control over residues 14-28, which are critical for PA pore-mediated protein translocation and blockage of ion conductance (13). To explore the roles of charged residues in this region, we replaced residues 14-28 with a peptide sequence devoid of charged residues, creating semisynthetic analog SSa2 (Figure 2). Another semisynthetic analog, SSa3, was prepared by replacing residues 14-28 with similar sequence, but containing 3 Lys residues at the N-terminus. The translocation properties of these semisynthetic LF_N analogues were characterized and found to be consistent with a charge state-dependent Brownian rachet model for translocation of LF_N through the pore (14).

The semisynthesis strategy we used to prepare LF_N^{14-263} and its analogues (Figure 3) involved two building blocks: chemically synthesized LF_N^{14-28} peptide-αthioester and recombinantly expressed N29C-LF_N^{29-263}. These two polypeptides were stitched together by native chemical ligation, producing N29C-LF_N^{14-263}. After the ligation reaction, purified N29C-LF_N^{14-263} was folded and then alkylated with 2-bromoacetamide to yield N29ψQ-LF_N^{14-263} (ψQ = pseudo-homoglutamine). Alkylation of Cys29 rendered the sulfhydryl less prone to oxidation and provided a native-like side chain at position 29, corresponding to Asn29 in the native structure.

LF_N^{14-28} αthioester was generated in two steps through adaptation of a procedure from Blanco-Canosa et al. that involves a C-terminal N-acyl-benzimidazolinone (Nbz) as a peptide thioester precursor (15). LF_N^{14-28} αNbz was prepared by Fmoc chemistry stepwise solid phase peptide synthesis (SPPS); after chain elongation was complete, the peptide was cleaved from the resin and side chain protection removed by treatment with trifluoroacetic acid and scavengers. Then, the crude peptide was transformed to LF_N^{14-28} αthioester by thiolysis with 4-mercraptophenylacetic acid (16). After overnight reaction, the product LF_N^{14-28} αthioester was purified and isolated by RP-HPLC. This procedure was used for all variant synthetic peptides.

N29C-LF_N^{29-263} was prepared from a His_6-SUMO-N29C-LF_N^{29-263} protein fusion construct (Figure S1) encoded by a pET15b-based plasmid. The fusion protein was isolated and purified on a Ni-NTA agarose resin. The product, His_6-SUMO-N29C-LF_N^{29-263}, was

treated with SUMO protease to generate the target recombinant N29C-LF_N^{29-263}, which was then purified by Ni-NTA agarose chromatography and RP-HPLC. A 5 liter *E. coli* growth yielded 195 mg pure lyophilized product. Alternative, recombinant routes were explored to prepare LF_N variants with an N-terminal Cys, which involved cyanogen bromide cleavage (17) or intein technology (IMPACT, New England Biolabs), but these routes gave much lower yields.

The analytical data for the native chemical ligation reaction used to prepare semisynthetic LF_N^{14-263} are shown in Figure 4. Lyophilized semisynthetic N29C-LF_N^{14-263} was dissolved in 6 M guanidine·HCl and then diluted to 1.5 M guanidine·HCl with 20 mM TRIS·HCl, pH 7, buffer containing 20 mM tris(carboxyethyl)phosphine·hydrochloride and 150 mM NaCl. The folded material was alkylated with 50 mM 2-bromoacetamide for 15 minutes, quenched with 100 mM 2-mercaptoethanesulfonate, and exchanged into 20 mM TRIS·HCl, pH 8.5, containing 150 mM NaCl. We isolated 2.5 mg (yield = 63%) of folded semisynthetic LF_N^{14-263} from 4 mg of starting material. The ESI-QTOF MS spectrum for purified semisynthetic analogues is shown in Figure 4. As a positive control, we subjected recombinant LF_N^{1-263} to the folding procedure and found no change in its interaction with PA pore in planar lipid bilayers. Recombinant LF_N^{1-263} has been reported to undergo reversible folding and unfolding (18). We found all semisynthetic analogues to have CD spectra identical, within experimental error, to that of recombinant LF_N^{1-263} (Figure S2), implying that they were correctly folded.

The semisynthetic LF_N analogues were characterized in planar phospholipid bilayers under voltage clamp conditions (10,19). A representative planar phospholipid bilayer experiment with PA pore and semisynthetic LF_N^{14-263} is shown in Figure 5a. A stable membrane was formed across a 200 μm hole by the brush technique (20), and PA prepore was added to picomolar concentrations to the cis compartment of the bilayer apparatus. Both compartments contained pH 5.5 buffer with 100 mM KCl, and the cis chamber was held at +20 mV with respect to the trans. As the cation-selective PA pores inserted into the membrane the current increased to a steady value of 100-500 picoamps, and residual PA in solution was then perfused from the chamber. When LF_N^{14-263} was added to the cis chamber, blockage of ion conductance occurred within seconds. After steady state conductance was reached, the unbound LF_N^{14-263} was removed by perfusion, and an aliquot of 2 M KOH was added to the trans compartment to create a pH gradient of 2 units. The pH gradient triggered translocation of LF_N through the PA pore, as indicated by an increase in ion conductance (14).

We compared the ion conductance block and translocation properties of the LF_N analogues, SSa1, SSa2, and SSa3, using this approach. All three analogues occluded the PA pore at low nanomolar concentrations (Figure 5b), whereas truncated N29C-LF_N^{29-263} did not, confirming that residues 14-28 at the N terminus of LF_N are required for LF_N to inhibit ion conductance through the pore (10). SSa3, the analogue with three positively charged residues and an acetylated N-terminus, blocked ion conductance more efficiently than the control analogue SSa2, which lacked charged residues in the N-terminal segment. We also carried out single-channel studies of pore occlusion and found the blocking characteristics of the LF_N^{14-263} variants to be similar to those seen in macroscopic studies (Figure S3).

Figure 5c displays the fraction of each LF_N variant translocated across the membrane as a function of time in response to raising the pH of the trans compartment. Semisynthetic LF_N^{14-263} (SSa1) translocated with efficiency similar to that of recombinant LF_N^{1-263}, whereas SSa2 and SSa3 were markedly defective in translocation. We found no significant differences between semisynthetic and recombinant forms of LF_N^{14-263}.

A net positive charge is believed to foster entry of the N terminus into the negatively charged pore lumen, where it interacts with the Phe clamp, a structure formed by the Phe427 residues, to block ion conductance (21). Consistent with this concept, we found that analog SSa3, which contains three Lys residues at the N-terminus, was highly efficient in blocking ion conductance, while SSa2, which has no charged residues in this region, was less efficient.

Once translocation has been initiated, propagation of the polypeptide through the pore can be driven by a pH gradient and has been proposed to occur by a charge state-dependent Brownian ratchet mechanism involving protonation and deprotonation of acidic side chains on the polypeptide (14). The pore is cation-selective, due to an electrostatic barrier in the pore that inhibits passage of negatively charged species, including negatively charged residues of a translocating polypeptide. Thus a proton gradient would bias diffusion of a polypeptide containing acidic residues towards the less acidic side of the membrane. We propose that both SSa2 and SSa3 failed to undergo translocation under the influence of a pH gradient because the absence of acidic residues in the residue 14-28 region interfered with the ratcheting process.

The properties of the semisynthetic analogues we constructed are thus consistent with the notion that the translocation of substrate proteins through the PA pore is dependent on the presence of both acidic and basic residues in the unstructured N-terminal region. These proof-of-principle findings serve to validate semisynthesis as a platform approach that will permit more varied and detailed studies of properties of proteins that affect their activities as substrates for translocation through the PA pore.

METHODS

Chemical Reagents

2-(1H-Benzotriazol-1-yl)-1,1,3,3-tetramethyluronium hexafluorophosphate (HBTU) and Nα-Fmoc protected amino acids (Peptide Institute) were obtained from Peptides International. N,N-Diisopropylethylamine (DIEA) was from Applied Biosystems. N,N-Dimethylformamide (DMF), dichloromethane (DCM), diethyl ether, HPLC-grade acetonitrile, and guanidine hydrochloride were purchased from Fisher. Trifluoroacetic acid (TFA) was from Halocarbon Products. All other reagents were purchased from Sigma-Aldrich.

Peptide Thioester Synthesis

Manual peptide synthesis was performed on a 0.4 mmol scale using previously reported protocols (15,22). Fmoc-Dbz was attached to Rink-PEG-PS resin (0.47 mmol/g) and after Fmoc removal standard chain elongation was performed. For each coupling reaction, 5 mL of solution containing 0.5 M HBTU (2.5 mmol) and 0.5 M Fmoc-Xaa (2.5 mmol) in DMF was added to the resin. Subsequently, 2.7 mmol of DIEA was added and the coupling reaction carried out for 30 minutes. The Fmoc protecting group was removed by treatment with 20 % (v/v) piperidine in DMF for 15 minutes. Side-chain protection for amino acids were as follows: Arg(Pbf), Lys(Boc), Asp(Obu^t), Glu(Obu^t), Asn(Trt). The last residue was incorporated as Boc-Lys(Boc), or the N-terminal was acetylated with acetic acid.

After completion of the chain assembly, the resin bound protected peptide was washed with DCM after which 20 mL of 50 mM *p*-nitrophenylchloroformate in DCM was added and allowed to stand for 40 minutes. The resin was washed with DCM and treated with two 10 mL portions of 0.5 M DIEA in DMF for 15 minutes. The resin was then washed with DMF, DCM, and dried under a stream of nitrogen. The peptides were cleaved from the resin support and side-chain protecting groups removed by treatment with trifluroacetic acid

(TFA) containing 2.5 % (v/v) H_2O and 2.5 % (v/v) triisopropylsilane. After 1 hour, the cleavage mixture was concentrated and the peptide was precipitated with diethylether and isolated by centrifugation.

The crude peptide mixture was dissolved in buffer containing 6 M guanidine·HCl, 20 mM tris(carboxyethyl)phosphine·hydrochloride (TCEP·HCl), 0.2 M phosphate, 100 mM 4-mercraptophenylacetic acid (MPAA) (16). The solution pH was adjusted to 7, allowed to react overnight, and the product peptide thioester purified by RP-HPLC.

The LF_N peptide thioesters and corresponding masses used for the semisynthesis were as follows: Ac-Lys^{14}-Lys-Lys-Ala-Gly-Ala-Asn-Ala-Gly-Ala-Asn-Ala-Gly-Ala-Gly^{28}-MPAA [observed (ob) 1477.73 ± 0.05 Da, calculated (ca) = 1477.43 Da (average isotopes)], Ac-Ala^{14}-Gly-Ala-Ala-Gly-Ala-Asn-Ala-Gly-Ala-Asn-Ala-Gly-Ala-Gly^{28}-MPAA [ob 1292.55 ± 0.05 Da, ca = 1292.11 Da (average isotopes)], Lys^{14}-Glu-Lys-Asn-Lys-Asp-Glu-Asn-Lys-Arg-Lys-Asp-Glu-Glu-Arg^{28}-MPAA [ob 2096.03 ± 0.05 Da, ca = 2096.11 Da (average isotopes)].

Plasmid preparation and recombinant protein expression

Recombinant WT PA was over-expressed in the periplasm of *E. coli* BL21 (DE3) and purified by anion exchange chromatography (23). LF_N^{1-263} was over-expressed in *E. coli* BL21 (DE3) and purified by affinity chromatography as previously described (10).

N29C-LF_N^{29-263} and K14G-LF_N^{14-263} were prepared by the use of Champion pET SUMO protein expression system (Invitrogen). Taq magic blue mix (Invitrogen) was used to PCR amplify N29C-LF_N^{29-263} from pET15b-LF_N^{1-263} by use of the a 5′-TGCAAAACACAGGAAGAGCATTTAAAGG-3′ (forward) and 5′-CTACCGTTGATCTTTAAGTTCTTCCAAGGATAGATTTATTTC-3′ (reverse) primer. The product identity was confirmed by 0.8 % (wt/vol) agarose gel electrophoresis and then desalted into 30 μL of water with Qiagen QIAquick PCR purification kit. The reaction was done in duplicate in which one reaction was used for gel analysis and the other was desalted and used for the ligation reaction. The desalted product was then cloned into pET SUMO by an overnight ligation at 15 °C with 1 μL of PCR product, 2 μL linear pET SUMO vector, 1 μL T4 DNA ligase in the supplied ligation buffer. The total volume was 10 μL. Then 2 μL of the ligation product was transformed into One Shot Mach1 -T1 competent cells and plated 50 μg/mL kanomycin plates and incubated overnight at 37 °C. Colonies were isolated and cultured overnight in LB media containing 50 μg/mL kanamycin. The plasmid DNA was isolated with Qiagen Qiaprep spin miniprep kit and sent for sequencing. The same procedure was used to prepare the K14G-LF_N^{14-263} pET15b SUMO plasmid except the following primers were used: 5′-GGTGAGAAA AATAAAGATGAGAATAAGAG-3′ (forward) and 5′-CTACCGTTGATCTTT AAGTTCTTCCAAGGATAGATTTATTTC-3′ (reverse) primer. N29C-LF_N^{29-263} and K14G-LF_N^{14-263} was over-expressed in *E. coli* BL21 (DE3) using 5 liter growths.

His_6-SUMO-N29C-LF_N^{29-263} cell pellets (200 g) were lysed by sonication in 200 mL of buffer containing 20 mM TRIS·HCl, 150 mM NaCl, one portion of Roche protease inhibitor cocktail, 10 mg of lysozyme, and 2 mg of DNAase I. The suspension was centrifuged at 15,000 rpm for 1 h to remove cell debris and filtered. The filtrate was loaded onto a Ni-NTA agarose column and washed with 500 mL of 20 mM TRIS·HCl, pH 8.5, 500 mM NaCl, and 20 mM imidazole. The protein was eluted from the column with buffer containing 500 mM imidazole, 20 mM TRIS·HCl, pH 8.5, and 500 mM NaCl. The fractions were analyzed by 4-12% TRIS Glycine SDS-PAGE and pooled. The product was exchanged into pH 8.5 buffer containing 20 mM TRIS·HCl and 150 mM NaCl. From 200 g of pellet we isolated 250 mg of His_6-SUMO-N29C-LF_N^{29-263}.

The pooled His_6-SUMO-N29C-LF_N^{29-263} was cleaved by SUMO protease treatment (1 μg protease per mg of protein) and after overnight reaction the mixture washed through a Ni-NTA agarose column to remove starting material and His_6-SUMO. The product was collected, purified by RP-HPLC, and lyophilized. Fractions were analyzed by SDS-PAGE and MALDI-TOF MS. The pooled material was reanalyzed with ESI-QTOF MS and observed mass was 27,284.94 ± 0.05 Da, ca = 27,284.90 Da (average isotopes). We obtained 195 mg of lyophilized N29C-LF_N^{29-263} using this procedure. The SDS-PAGE analysis for the preparation of N29C-LF_N^{29-263} is shown in Figure S1.

Analytical HPLC

Peptide compositions were confirmed by analytical reverse phase LC on a Agilent 1200 using a gradient of acetonitrile versus 0.1% trifluoroacetic acid (TFA) in water. For the work reported in this paper, analytical HPLC was carried out as follows: Phenomenex Jupiter C5 4.6 × 250 mm column using a linear gradient of 5-70 % buffer B over 23 min at 23 °C with a flow rate of 1.0 mL/min (buffer A= 0.1% TFA in H2O; buffer B = 0.08% TFA in acetonitrile). The effluent was monitored at 214 nm.

Analytical MS

All peptide thioesters and semisynthetic products were analyzed on a Agilent 6520 accurate-mass quadrupole time-of-flight (ESI-QTOF MS). A desalt gradient of acetonitrile versus 0.1% formic acid in water was used for MS analysis. LC-MS used a Grace Vydac C4 2.1 × 100 mm column using a linear gradient of 1-71 % buffer B over 15 min with a flow rate of 0.5 mL/min (buffer A= 0.1% formic acid in H2O; buffer B = 0.1% formic acid in acetonitrile) at 40 °C. The observed mass spectrum was generated by averaging over the major peak in the total ion chromatogram.

Preparative HPLC

Peptides were purified on C18 Phenomenex jupiter using a column of dimension 10 × 250 mm. Crude peptides were loaded onto the prep column in ~1% acetonitrile/99% (0.1%TFA in water), and eluted at a flow rate of 5 mL per minute with a shallow gradient (e.g. 20%B-40%B over 60 minutes) of increasing concentrations of solvent B (0.1% TFA in acetonitrile) in solvent A (0.1% TFA in water). LF_N constructs were purified on C4 TP Grace Vydac silica with column of dimension 10 × 250 mm. Fractions containing the pure target peptide were identified by analytical LC, SDS-PAGE electrophoresis, MALDI-TOF MS, and were combined and lyophilized. The pooled material was reanalyzed on a ESI-QTOF MS before use.

Native chemical ligation

Ligation reactions were carried out under previously published conditions (16): 0.6 mL of 200 mM sodium phosphate buffer containing 6 M guanidine·HCl, 40 mM TCEP·HCl, pH = 6.8, ~2 mM for each peptide, 20 mM MPAA, purged and sealed under argon. After purification and lyophilization the following amounts of each analogue were obtained: 0.5 micromole of N29C-LF_N^{14-263} (15 mgs, 43% yield), 0.3 micromole of N29C-SSa2 (9.2 mgs, 27% yield), and 0.5 micromole of N29C-SSa3 (14.4 mgs, 43% yield).

Protein folding and alkylation

For semisynthetic N29C-LF_N^{14-263}, the HPLC purified product was folded by dissolving 4 mg in 100 μL of 6 M guanidine·HCl and then diluting to 1.5 M guanidine·HCl by the addition of 300 μL of pH = 7 buffer containing 20 mM TRIS·HCl, 20 mM TCEP·HCl, and 150 mM NaCl. Then 3 mg of 2-bromoacetamide (50 mM) was added and allowed to stand for 15 minutes. The residual 2-bromoacetamide was quenched by the addition of 7 mg of

sodium 2-mercaptoethanesulfonate (100 mM). The reaction was desalted on a 5 mL HiTrap desalt column into pH 8.5 buffer containing 20 mM TRIS·HCl and 150 mM NaCl. After folding and alkylation we isolated 2.55 mg (64%) of N29ψQ-LF_N^{14-263}. For the other analogues, starting with approximately half as much material as for N29C-LF_N^{14-263}, we obtained SSa2 (0.4 mgs, 20%), and SSa3 (0.6 mg, 50%)

Macroscopic planar phospholipid bilayer studies

Planar phospholipid bilayers were formed by painting (20) with 35 mM 1,2-diphytanoyl-sn-glycerol-3-phosphocholine (DPhPC, Avanti Polar Phospholipids) in n-decane onto a Delrin cup with a μ200 m aperture in a Lucite chamber. Both compartments contained 1 mL of pH 5.6 buffer containing 100 mM KCl, 1 mM ethylenediaminetetraacetic acid, 10 mM sodium oxalate, 10 mM potassium phosphate, and 10 mM 2-(N-morpholino)ethanesulfonic acid. PA prepore and LF_N analogues were added to the cis chamber and trans refers to the side of 2 M KOH addition. The membrane potential, Δψ, is defined as Δψ=ψcis–ψtrans, where ψtrans ≡ 0 mV.

Once a membrane was formed in the planar phospholipid bilayer system, PA prepore (~1 pM) was added to the cis compartment, held at +20 mV with respect to the trans compartment. The chambers were stirred continuously except when perfusing. Once the current stabilized, the cis compartment was perfused with 5 mL of non-PA-containing buffer. Then a LF_N analogue was added to the cis compartment and the progress of binding to PA channels was monitored by the fall in conductance. The cis compartment was perfused again with 5-12 mL of buffer depending on the analogue tested. Translocation was initiated by raising the pH of the trans compartment to pH 7.6 with 2 M KOH, while maintaining the cis compartment pH at 5.6. All experiments were monitored at a +20 mV. Experiments were carried out at least 3 times.

The current blockage (%) was calculated by using the equation $I_{cb} = (I_b/ I_o) \times 100$, where I_b is the steady state current after LF_N addition and I_o is the current LF_N addition. Translocation fraction using the equation $F_u = (I_t - I_c)/ (I_o - I_c)$, where F_u is fraction translocated, I_t is the instantaneous current after the addition of KOH, I_c is the current of blocked channels after the addition of LF_N and perfusion, and I_o is the steady state current of open channels after perfusion of PA pore.

Supplementary Material

Refer to Web version on PubMed Central for supplementary material.

Acknowledgments

This research was supported by NIAID grants RO1-AI022021 and AI057159. RJC holds equity in PharmAthene, Inc. The recombinant proteins employed in the study were prepared in the Biomolecule Production Core of the New England Regional Center of Excellence, supported by NIH grant number AI057159. We thank R. Ross, L. Perry, and their staff for these services. We thank R. Melynk and B. Krantz for suggesting in early discussions that native chemical ligation be used to study lethal toxin. We thank D. Bang, A. Fischer, L. Jennings, and O. Sharma for valuable comments and discussions, and S. Walker and E. Doud for providing access to their ESI-QTOF MS.

REFERENCES

1. Young JA, Collier RJ. Anthrax toxin: receptor binding, internalization, pore formation, and translocation. Annu Rev Biochem 2007;76:243–265. [PubMed: 17335404]
2. Bradley KA, Mogridge J, Mourez M, Collier RJ, Young JA. Identification of the cellular receptor for anthrax toxin. Nature 2001;414:225–229. [PubMed: 11700562]

3. Scobie HM, Rainey GJ, Bradley KA, Young JA. Human capillary morphogenesis protein 2 functions as an anthrax toxin receptor. Proc Natl Acad Sci U S A 2003;100:5170–5174. [PubMed: 12700348]
4. Molloy SS, Bresnahan PA, Leppla SH, Klimpel KR, Thomas G. Human furin is a calcium-dependent serine endoprotease that recognizes the sequence Arg-X-X-Arg and efficiently cleaves anthrax toxin protective antigen. J Biol Chem 1992;267:16396–16402. [PubMed: 1644824]
5. Klimpel KR, Molloy SS, Thomas G, Leppla SH. Anthrax toxin protective antigen is activated by a cell surface protease with the sequence specificity and catalytic properties of furin. Proc Natl Acad Sci U S A 1992;89:10277–10281. [PubMed: 1438214]
6. Milne JC, Furlong D, Hanna PC, Wall JS, Collier RJ. Anthrax protective antigen forms oligomers during intoxication of mammalian cells. J Biol Chem 1994;269:20607–20612. [PubMed: 8051159]
7. Kintzer AF, Thoren KL, Sterling HJ, Dong KC, Feld GK, Tang II, Zhang TT, Williams ER, Berger JM, Krantz BA. The protective antigen component of anthrax toxin forms functional octameric complexes. J Mol Biol 2009;392:614–629. [PubMed: 19627991]
8. Abrami L, Liu S, Cosson P, Leppla SH, van der Goot FG. Anthrax toxin triggers endocytosis of its receptor via a lipid raft-mediated clathrin-dependent process. J Cell Biol 2003;160:321–328. [PubMed: 12551953]
9. Abrami L, Lindsay M, Parton RG, Leppla SH, van der Goot FG. Membrane insertion of anthrax protective antigen and cytoplasmic delivery of lethal factor occur at different stages of the endocytic pathway. J Cell Biol 2004;166:645–651. [PubMed: 15337774]
10. Zhang S, Finkelstein A, Collier RJ. Evidence that translocation of anthrax toxin's lethal factor is initiated by entry of its N terminus into the protective antigen channel. Proc Natl Acad Sci U S A 2004;101:16756–16761. [PubMed: 15548616]
11. Muir TW. Studying protein structure and function using semisynthesis. Biopolymers 2008;90:743–750. [PubMed: 18924136]
12. Dawson PE, Muir TW, Clark-Lewis I, Kent SB. Synthesis of proteins by native chemical ligation. Science 1994;266:776–779. [PubMed: 7973629]
13. Zhang S, Udho E, Wu Z, Collier RJ, Finkelstein A. Protein translocation through anthrax toxin channels formed in planar lipid bilayers. Biophys J 2004;87:3842–3849. [PubMed: 15377524]
14. Krantz BA, Finkelstein A, Collier RJ. Protein translocation through the anthrax toxin transmembrane pore is driven by a proton gradient. J Mol Biol 2006;355:968–979. [PubMed: 16343527]
15. Blanco-Canosa JB, Dawson PE. An efficient Fmoc-SPPS approach for the generation of thioester peptide precursors for use in native chemical ligation. Angew Chem Int Ed Engl 2008;47:6851–6855. [PubMed: 18651678]
16. Johnson EC, Kent SB. Insights into the mechanism and catalysis of the native chemical ligation reaction. J Am Chem Soc 2006;128:6640–6646. [PubMed: 16704265]
17. Macmillan D, Arham L. Cyanogen bromide cleavage generates fragments suitable for expressed protein and glycoprotein ligation. J Am Chem Soc 2004;126:9530–9531. [PubMed: 15291543]
18. Krantz BA, Trivedi AD, Cunningham K, Christensen KA, Collier RJ. Acid-induced unfolding of the amino-terminal domains of the lethal and edema factors of anthrax toxin. J Mol Biol 2004;344:739–756. [PubMed: 15533442]
19. Blaustein RO, Koehler TM, Collier RJ, Finkelstein A. Anthrax toxin: channel-forming activity of protective antigen in planar phospholipid bilayers. Proc Natl Acad Sci U S A 1989;86:2209–2213. [PubMed: 2467303]
20. Mueller P, W W, Rudin DO, Tien HT. Methods for formation of single biomolecular lipid membranes in aquesous solution. Jounral of Physical Chemistry 1963;67:534–535.
21. Krantz BA, Melnyk RA, Zhang S, Juris SJ, Lacy DB, Wu Z, Finkelstein A, Collier RJ. A phenylalanine clamp catalyzes protein translocation through the anthrax toxin pore. Science 2005;309:777–781. [PubMed: 16051798]
22. Schnolzer M, Alewood P, Jones A, Alewood D, Kent SB. In situ neutralization in Boc-chemistry solid phase peptide synthesis. Rapid, high yield assembly of difficult sequences. Int J Pept Protein Res 1992;40:180–193. [PubMed: 1478777]

23. Miller CJ, Elliott JL, Collier RJ. Anthrax protective antigen: prepore-to-pore conversion. Biochemistry 1999;38:10432–10441. [PubMed: 10441138]

24. Katayama H, Janowiak BE, Brzozowski M, Juryck J, Falke S, Gogol EP, Collier RJ, Fisher MT. GroEL as a molecular scaffold for structural analysis of the anthrax toxin pore. Nat Struct Mol Biol 2008;15:754–760. [PubMed: 18568038]

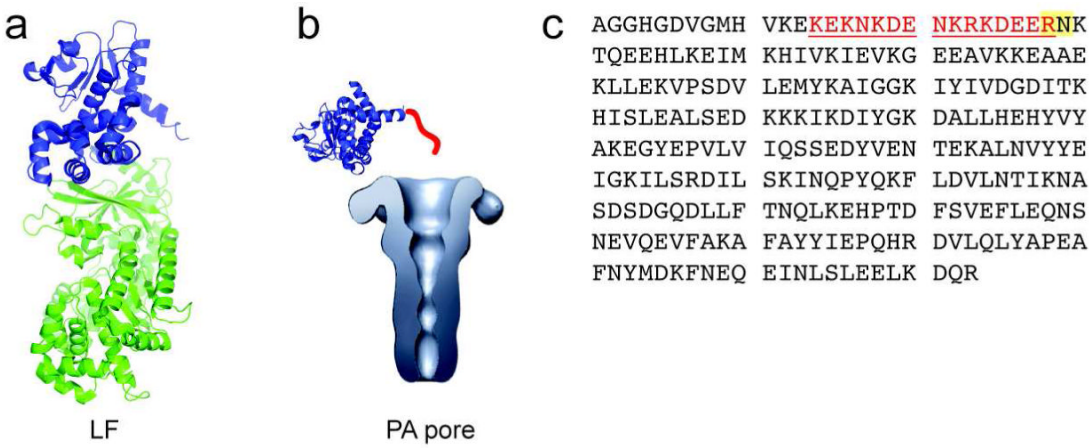

Figure 1.

N-terminal domain of Lethal Factor. a) Xray structure of Lethal Factor with the N-terminal PA binding domain highlighted in blue (PDB 1J7N). b) Binding interaction of the N-terminal Lethal Factor domain with the PA pore, the latter structure having been reconstructed from single-pore images obtained by electron microscopy (24). Highlighted in red is the N-terminal stretch needed for translocation. This region was not present in the Xray structure. c) The amino acid sequence of Lethal Factor N-terminal domain (LF_N^{1-263}) with residues 14-28 highlighted in red and the ligation site highlighted in yellow.

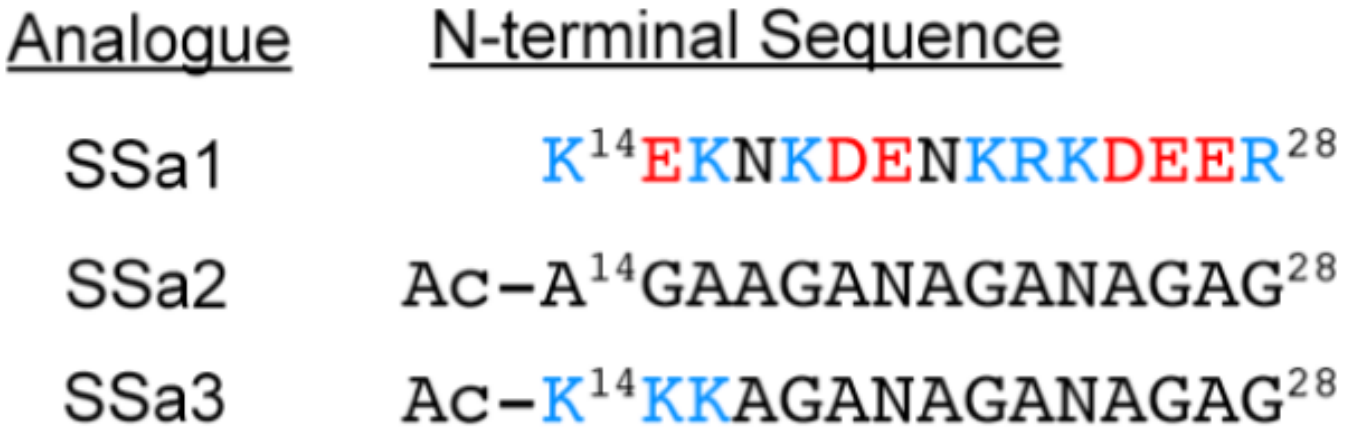

Figure 2.
Analogues prepared for the investigation of the N-terminal $LF_N^{14\text{-}263}$ sequence (Ac = acetyl).

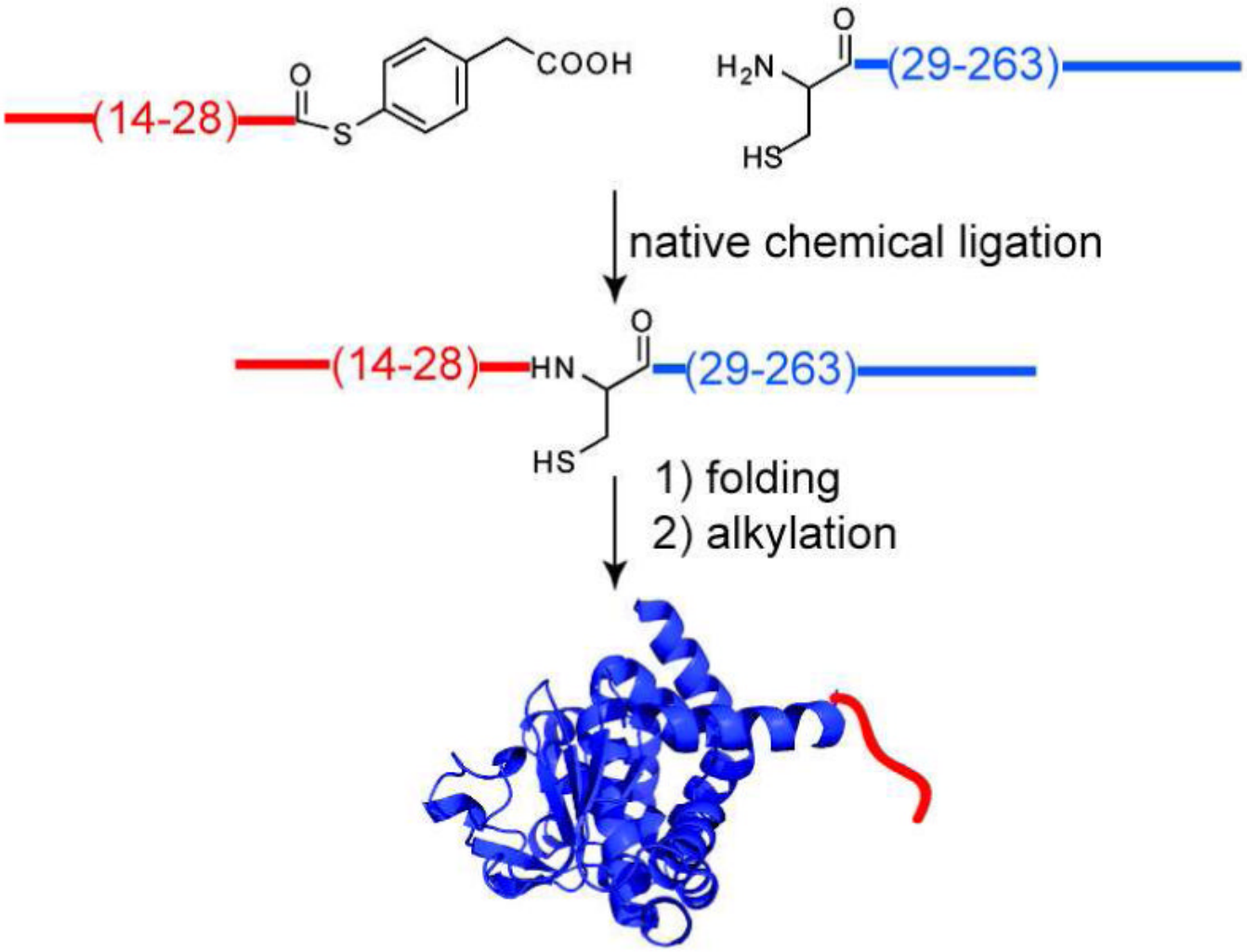

Figure 3.
Semisynthesis strategy involving native chemical ligation to vary the N-terminal sequence of LF_N.

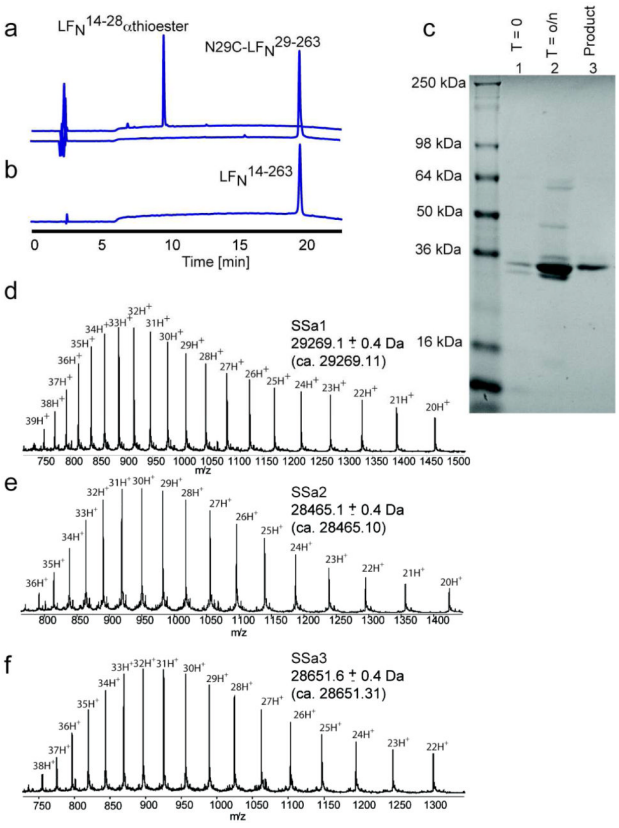

Figure 4.

Physical-chemical characterization of LF_N^{14-263} and analogues. Analytical LC of the purified starting materials (a) and purified reaction product (b). The effluent was monitored at λ = 214 nm. c) SDS-PAGE analysis of the ligation reaction. The gel was stained with Coomassie Brillliant Blue. d-f) ESI-QTOF MS data for the purified, folded, and alkylated semisynthetic LF_N analogues. The analytical details are reported in the experimental section.

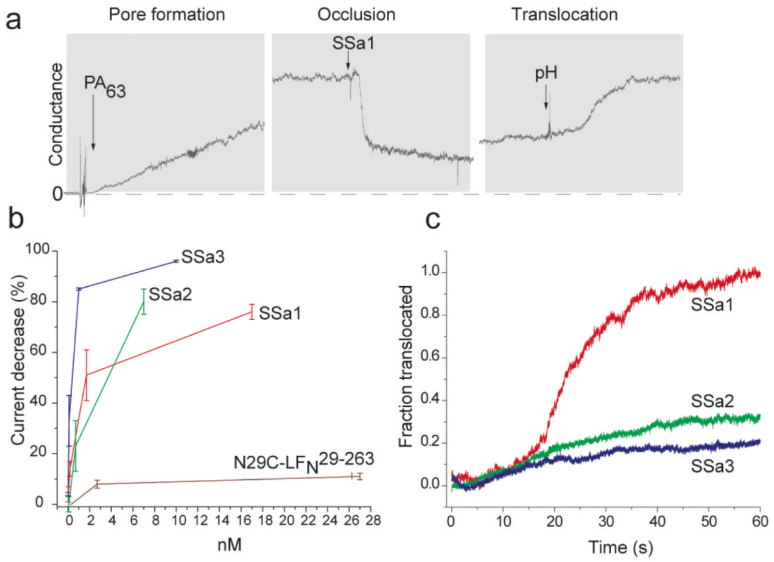

Figure 5.

Macroscopic planar phospholipid bilayer characterization of LF_N analogues under an applied membrane potential of 20 mV. a) Representative planar phospholipid bilayer experiment for semisynthetic LF_N^{14-263} and PA pore. b) Percent ion conductance block of PA pore as a function of the concentration of semisynthetic LF_N analogues. Each experiment was repeated three times. c) The fraction of LF_N variants translocated across the phospholipid bilayer as a function of time in response to a pH gradient of ~2 units.